hydrogen

MDPI

Review

Effect of Ti-Based Additives on the Hydrogen Storage Properties of MgH_2: A Review

Mukesh Jangir [1], Indra Prabh Jain [2] and Daniele Mirabile Gattia [3,*]

[1] School of Applied Science and Technology, NIMS University, Jaipur 303121, India; mukesh.kumari@nimsuniversity.org
[2] Centre for Non-Conventional Energy Resources, University of Rajasthan, Jaipur 302004, India; ipjain46@gmail.com
[3] Department for Sustainability, ENEA Casaccia Research Center, Via Anguillarese 301, 00123 Rome, Italy
* Correspondence: daniele.mirabile@enea.it

Abstract: For the few past decades, study of new hydrogen storage materials has been captivating scientists worldwide. Magnesium hydride, MgH_2, is considered one of the most promising materials due to its low cost, high hydrogen capacity, reversibility and the abundance of Mg. However, it requires further research to improve its hydrogen storage performance as it has some drawbacks such as poor dehydrogenation kinetic, high operational temperature, which limit its practical application. In this study, we introduce an overview of recent progress in improving the hydrogen storage performance of MgH_2 by the addition of titanium-based additives, which are one of the important groups of additives. The role of Ti-based additive hydrides, oxides, halides, carbides and carbonitrides are overviewed. In addition, the existing challenges and future perspectives of Mg-based hydrides are also discussed.

Keywords: hydrogen storage; magnesium hydride; titanium-based additives

check for updates

Citation: Jangir, M.; Jain, I.P.; Mirabile Gattia, D. Effect of Ti-Based Additives on the Hydrogen Storage Properties of MgH_2: A Review. *Hydrogen* **2023**, *4*, 523–541. https://doi.org/10.3390/hydrogen4030034

Academic Editor: Jacques Huot

Received: 16 June 2023
Revised: 29 July 2023
Accepted: 1 August 2023
Published: 5 August 2023

1. Introduction

The rapidly increasing consumption of energy is depleting limited fossil fuel supplies and the world is facing the problem of energy resource scarcity and other environmental problems [1]. Moreover, burning of fossil fuels is one of the main causes of the greenhouse effect that is an actual environmental issue. In this scenario, sustainable energy resources and high-efficiency energy systems, which can meet the requirement of clean energy and sustainable growth, are required [2]. Hence, the development of renewable energy proceeds fast and new drivers are considered as an environmentally friendly solution, such as hydrogen energy. In the last few decades, the importance of hydrogen energy has been proposed, but still now researchers investigate how hydrogen can be used more significantly and lead to a more sustainable environment [3]. However, storing hydrogen remains challenging and some issues have to be taken into account such as safety, compactness, lightness, cycling and cost of the storage system [4].

Solid hydrogen storage is a suitable alternative to compressed gas storage and cryogenic liquid storage. There are two types of sorption mechanism to store hydrogen in materials, physisorption and chemisorption [5]. Earlier studies reveal that magnesium hydride, MgH_2, is one of the most suitable candidates for storing hydrogen due to its low density, high hydrogen capacity (7.6 wt%), high abundance, low cost, good heat resistance, vibration absorption, reversibility and recyclability. Nevertheless, it suffers some limitations due to sluggish absorption/desorption kinetics and the elevated temperature required for hydrogen absorption and desorption [4].

Different approaches have been investigated by researchers to alleviate the above limitations, such as nano-structuring [6–9], alloying [10–12] and the addition of a catalyst [13–15].

The effect of high energy milling on MgH_2 was investigated by TEM observations and analyses by M. Danaie et al. [16]. The authors found a reduction of the activation energy due to deformation of twinning in MgH_2. Kinetics of MgH_2 are notably enhanced by the addition of a transition metal, halides and oxides and carbon material by the reduction of the metal−hydrogen bond energy and by lowering of the decomposition temperature. Among them, because of the high affinity of the transition metal cation towards hydrogen, transition metal compounds are highly effective catalysts [17,18]. Transition metals promote the dissociation and re-combination of hydrogen and the kinetics are improved by the addition of small amounts of such material. In one of the studies, M. Danaie observed that ball milled MgH_2 and Fe particles form Mg_2FeH_6 during the process of thermal hydrogenation. Fe particles behave as a catalyst and dissociate the molecular hydrogen to form atomic hydrogen [19]. The effect of few at% Fe on the hydrogenation of MgH_2 thin film was also observed by some researchers and results showed the significant improvement of the hydride phase growth rate. Reduction in absorption/desorption entropy and enthalpy were also noticed [20].

B. Zahiri et al. studied the hydrogenation properties of Mg-15 at% Fe-15Ti, Mg10 at% Fe-10Ti and Mg-Ti-Cr thin films [21]. The authors observed that 5 wt% of hydrogen is absorbed by these thin films within seconds and desorbed in minutes at 250 °C. N. Hanada et al. [18] observed that 3d-transition metal (Fe, Co, Cu, Ni) doped MgH_2, prepared by milling, presents improved hydrogen desorption properties with respect to pure ball-milled MgH_2. Among these transition metals, Ni shows a better catalytic effect and MgH_2 desorbs 6.5 wt% of hydrogen in the temperature range 150–250 °C. H. Gasan et al. [22] investigated the effect of the addition of 5 wt% of Ti, V, Nb and graphite on the dehydrogenation temperature and reported that these additives cause a reduction of the desorption temperature of about 40–50 °C compared with that of as-received MgH_2.

Due to its properties, as a lightweight and low cost material, Ti captivates scientists' attention. Ti acts as a catalyst and it exhibits a strong affinity for hydrogen even at moderate temperatures, improving the hydrogenation/dehydrogenation kinetics in several hydrogen storage systems [23]. The addition of catalysts provides a crucial track to enhance surface kinetics. In this paper, the use of Ti as an additive for hydrogenation/dehydrogenation of MgH_2 is reviewed.

2. Fundamentals of the MgH_2 System

2.1. Crystal Structure of MgH_2 System

MgH_2 is a hexagonal-close packed and stoichiometric compound with a H/Mg atomic ratio of 0.99 ± 0.01 [24] and density of 1.74 g/cm^3. Magnesium reacts with hydrogen under different conditions and forms different types of structures. During absorption, firstly the hydrogen molecule dissociates on the Mg particles surface. Hydrogen atoms initially occupy tetrahedral interstitial sites to form an α phase. The structure of α-MgH_2 is a tetragonal Rutile type. Under high pressure, α-MgH_2 undergoes polymorphic transformation to form two modifications: γ-MgH_2 and β-MgH_2 having an orthorhombic [25] and a hexagonal structure, respectively [26]. According to Varin et al., high energy ball milling of MgH_2 results in the formation of both γ- and β-MgH_2 phases, and the presence of these metastable phases lowers the desorption temperature. In Figure 1 the crystal structure of MgH_2 is reported [27].

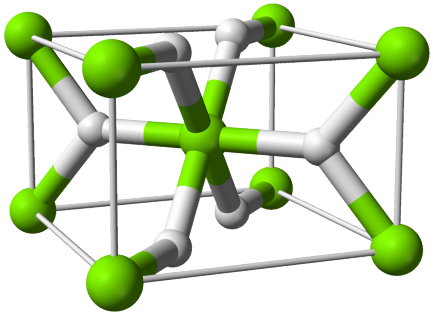

Figure 1. Crystal structure of MgH_2 [27].

In Table 1, different crystalline MgH_2 phases and their crystal parameters are reported [28].

Table 1. Structural parameters for MgH_2 in ambient and high-pressure phases. (Reprinted with permission from ref. [28]. Copyright 2006 American Physical Society.)

Structure Type	Unit Cell (Å)			Positional Parameters	B_O (GPa)	B_o
	A	B	C			
β-MgH_2	4.5176	4.5176	3.0206	Mg(2a), 0, 0, 0	45.00 ± 2	3.35 ± 0.3
γ-MgH_2	4.6655	4.6655	4.6655	Mg(4a), 0, 0, 0	47.41 ± 4	3.39 ± 0.4
α-MgH_2	4.5248	5.442	4.9285	Mg(4c), 0, 0, 0	44.03 ± 2	3.17 ± 0.4
δ-MgH_2	8.8069	4.6838	4.3699	Mg(4c), 0.8823, 0.271, 0.2790	49.83 ± 5	3.49 ± 0.6

2.2. Thermodynamics of the MgH_2 System

Stampfer et al. [24] for the first time evaluated the thermodynamic properties of MgH_2 and reported its enthalpy (−74.5 kJ/mol·H_2) and entropy (136 J/K·mol·H_2) of formation. Thermodynamic behaviour of a hydride can be explained by pressure composition isotherms, representing the pressure vs. hydrogen to metal ratio at a constant temperature. Reporting the plateau pressures in the Van't Hoff plot, the enthalpy and the entropy are respectively determined by the slope and the intercept of the linear fit (Figure 2 [29]).

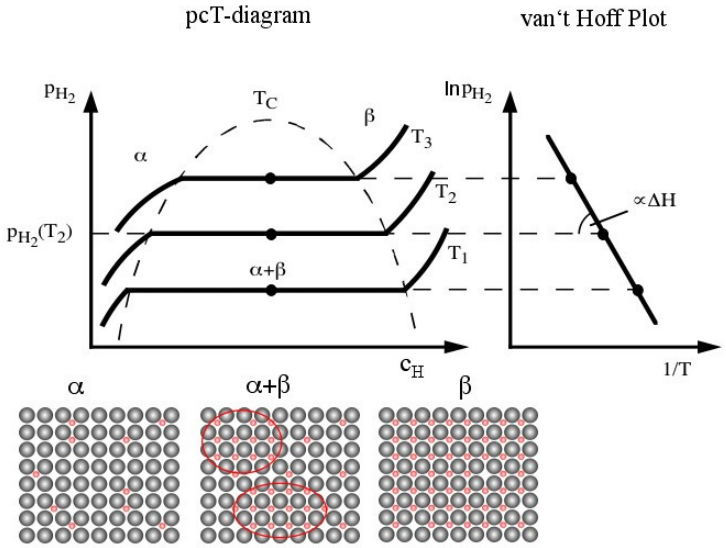

Figure 2. Schematic pressure composition isotherm and Van't Hoff plot [29].

In terms of thermodynamic properties, suitable materials for solid hydrogen storage should have a bonding enthalpy in the range 25–45 kJ/mol·H_2 [30]. Hence, many efforts have been done to remove constraints and lower the ΔH, which are important for on-board application. Some methods were suggested such as alloying, downsizing and the stress effect. In Figure 3, the alloying formation of stable Mg compounds with other elements, such as Mg_2Si, Mg_2Ca, Mg_2NiH_4, Mg_2FeH_6 is reported [31–34]. Mg-Ti-H systems have been investigated but, due to immiscibility, no compounds can be formed between Mg and Ti. K. Asano et al. [35] reported hexagonal close-packed, face-centred cubic and body-centred cubic Mg_xTi_{100-x} ($35 \leq x \leq 80$) alloys, obtained by ball milling. P. Vermeulen et al. [36] investigated the extremely low plateau pressure (≈10^{-6} bar at room temperature) in the Mg-Ti-H system. When it forms ternary composite with Al or Si a higher plateau pressure can be observed and its hydrogen capacity increases until 6 wt%.

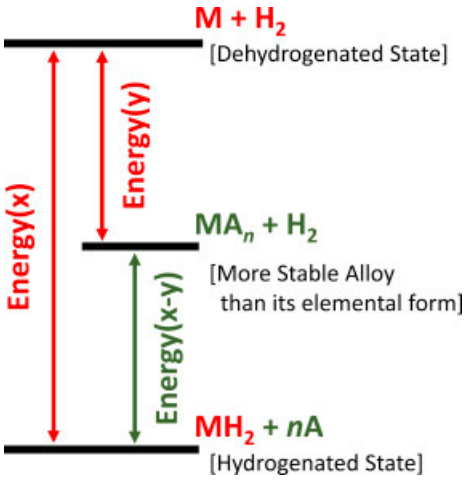

Figure 3. Schematic representation of destabilisation mechanism kinetics (Copyright Elsevier 2016 [37]).

2.3. Kinetics of MgH_2 System

In order to store hydrogen in metals in the atomic form or through chemical reactions involving hydrogen, molecular hydrogen must first be split into hydrogen moieties during chemical storage. Hydrogen reacts with metal and forms stronger bonds whereas, in physisorption, hydrogen is weakly adsorbed on the metal surface. When atomic hydrogen reacts with other atoms, or molecules, it either gains or loses an electron, depending on the electronegativity of the other metal atom or molecule. In the case of electropositive metals, such as alkali or alkaline earth metals, atomic hydrogen gains an electron and it forms an ionic hydride; on the other hand, in the case of an electronegative atom or molecule (p-block elements, such as boron and nitrogen), the hydrogen atom exists as a proton. Hydrogen absorption reaction consists of several different steps [38,39].

(i) Surface assimilation of molecular hydrogen:

Physisorption of an H_2 molecule on a metal surface requires extremely little activation energy, it is not commonly seen as a limiting step. The remaining steps may be rate limiting, which is worth debating.

(ii) Hydrogen molecules convert into atoms:

Both theoretical calculations and experimental results indicate that a significant energy barrier must be overcome when hydrogen dissociates on a pure Mg surface. According to Du et al. [40], the hydrogen dissociation activation barrier decreases from 1.051 eV for a pure Mg(0001) surface to 0.103 eV and 0.305 eV for Ti-doped and Pd-doped Mg(0001) surfaces, respectively.

Once the hydrogen molecules dissociate into atoms on the surface, an obstacle may still exist to prevent transfer of hydrogen atoms from catalytic sites into the bulk. The so-called "hydrogen spillover" mechanism may play the role in Mg-TM catalysed systems [41].

(iii) Penetration of hydrogen atoms on the surface:

Surface modification is required to increase dehydrogenation and hydrogenation kinetics due to the presence of a surface oxide layer, which prevents hydrogen atoms from penetrating into the bulk. Even in an inert gas with a trace amount of O_2/H_2O, the continuous passive $MgO/Mg(OH)_2$ layer would easily cover the Mg/MgH_2 surface [42].

Recent research on the effect of air exposure on $TiMn_2$ catalysed MgH_2 [43] found that direct air exposure reduces the hydrogen storage capacity while only causing modest kinetic degradation. Further surface characterisation revealed that MgH_2 forms a layer with $Mg(OH)_2$ and MgO. The layer may shatter during hydrogen cycling, however, the nanocomposite can be reactivated in the presence of a catalyst. The doped catalyst particles

on hydride surfaces can act as pathways for hydrogen to be transferred from the surface to the bulk, or from MgH_2 to the outside. As asserted in MgH_2-Nb [44] and MgH_2-Pt [45] catalysed systems, this mechanism is known as the "hydrogen gateway" effect.

(iv) Diffusion of atomic hydrogen:

The use of a catalyst could help to accelerate the rate of hydrogen diffusion in the matrix. Because MgH_2 has a sluggish diffusion rate, it is expected that the reaction will switch to diffusion control when the developing hydride covers the particles during hydrogenation. Nano-doped catalytic species are thought to expedite hydrogen diffusion in both hydrogenation and dehydrogenation processes. This mechanism is commonly referred to as the "hydrogen pathway" effect.

(v) Formation of hydride at the metal/hydride interface:

The final step in the hydrogenation of Mg is the nucleation and development of the MgH_2 phase. Because of the crystal structural difference between Mg metal and its developing hydride, the nucleation and growth of a hydride phase will result in significant interfacial energy shifts. It is still debated whether the rate-limiting stage is controlled by nucleation and growth or hydrogen diffusion.

Desorption takes place via a reverse reaction. In most cases, hydride nucleation and growth or diffusion are rate determining steps for desorption kinetics [39]. In general, H_2 molecule dissociation requires an additional amount of energy, known as the activation energy. Experiments for kinetic studies of metal hydride are carried out under isothermal and non-isothermal conditions.

Generally, a Sievert-type apparatus is used for isothermal kinetic study, which permits us to find a precise volumetric measurement of the amount of hydrogen released at appropriate pressure and temperature. In order to obtain comprehensive information about the dehydrogenation/hydrogenation kinetics, the activation energy (E_a) for a reaction is calculated using the Arrhenius equation, which combines the concept of activation energy with a Boltzmann distribution law [31].

$$k(T) = A \exp(-E_a/RT)$$

where k(T) is the reaction-rate constant; A is a pre-exponential factor; E_a is the activation energy for the reaction; R is the ideal gas constant; T is the absolute temperature.

Under non-isothermal conditions, thermogravimetric analysis is used. It allows us determine the weight loss as a function of temperature. The changes in thermal characteristics are represented by a deflection or peak in the curve. The fluctuation in peak temperature can be used to calculate the activation energy of first order processes. The activation energies are evaluated by plotting a curve between lnK and $1/RT_P$ using the following equation:

$$\ln k = -E_a/RT_p + a$$

where

$k = \beta/T_p^2$;
β = heating rate;
T_p = peak temperature;
E_a = activation energy of desorption;
R = gas constant.

3. Effect of Catalyst

To improve the kinetics of hydrogen absorption and desorption reactions of magnesium-based materials, the addition of catalysts or additives and nano-structuring are two important approaches.

3.1. Transition Metal Catalyst or Additives

Among all the additives, the transition metal (TM)-based catalyst shows significant improvement in the kinetics without sacrificing the hydrogen storage capacity. The effect of various TM-based catalysts on the hydrogenation/dehydrogenation properties of MgH_2 have been intensively investigated.

The addition of a small amount of these catalysts improved the kinetics of MgH_2 as these facilitate the dissociation and recombination of hydrogen. Liang et al. [17] studied the effect of TM (as Ti, V, Mn, Fe and Ni) on the hydrogenation properties of ball milled MgH_2. No change in entropy and enthalpy but a reduction in activation energy of desorption for magnesium hydride were reported. The activation energies (E_a) of MgH_2-V, MgH_2-Ti, MgH_2-Ni, MgH_2-Fe and MgH_2-Mn are evaluated to be 62.3. kJ/mol, 71.1 kJ/mol, 88.1 kJ/mol, 67.6 kJ/mol and 104.6 kJ/mol, respectively, which are significantly reduced compared to that of the ball-milled pure MgH_2 (120 kJ/mol).

Among them, MgH_2–V and MgH_2–Ti show the fastest desorption at low temperatures. Study of mechanically milled MgH_2 with 5 wt.% of additives (V, Nb, Ti and graphite) showed a reduction of the hydrogen desorption temperature by about ~40–50 °C compared with that of as-received MgH_2 [22]. In another study, Zhou et al. found that elements of the IV-A and V-A groups are the most effective additives. Elements of VII-A (Mn), VIII-A (Fe, Co, Ni) have a moderate effect and Mo, Mo oxides and W oxide Yttrium (III-A group) and Yttrium oxide showed no improvement in the kinetics. MgH_2 with Ti has the lowest onset temperature followed by V, Mn, Zr, Nb, Fe, Ni, Cr and Co. In Figure 4, the effect of different additives on the desorption temperature of MgH_2 is reported, as reprinted from [46], while in Figure 5 the desorption curves of MgH_2–5 at%Tm (Tm = Ti, V, Mn, Fe and Ni) composites under a hydrogen pressure of 0.015MPa and different temperatures are reported [17].

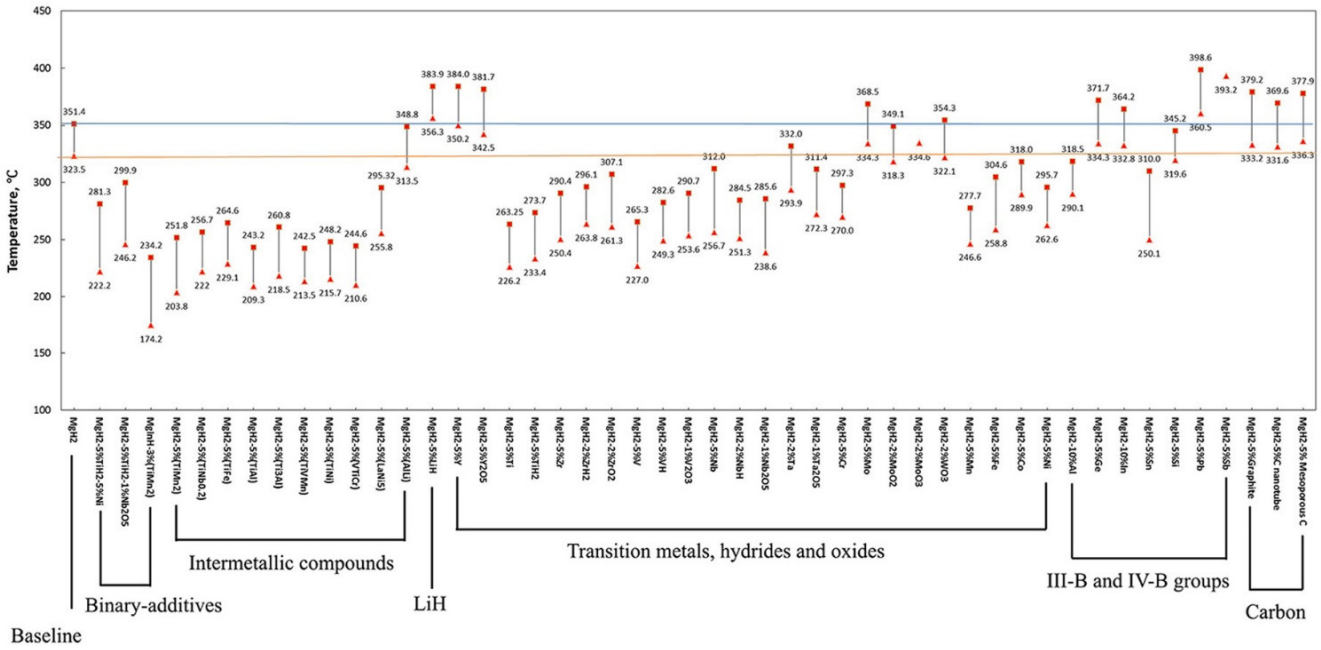

Figure 4. Effect of different additives on desorption temperature of MgH_2 (Copyright Elsevier 2015 [46]).

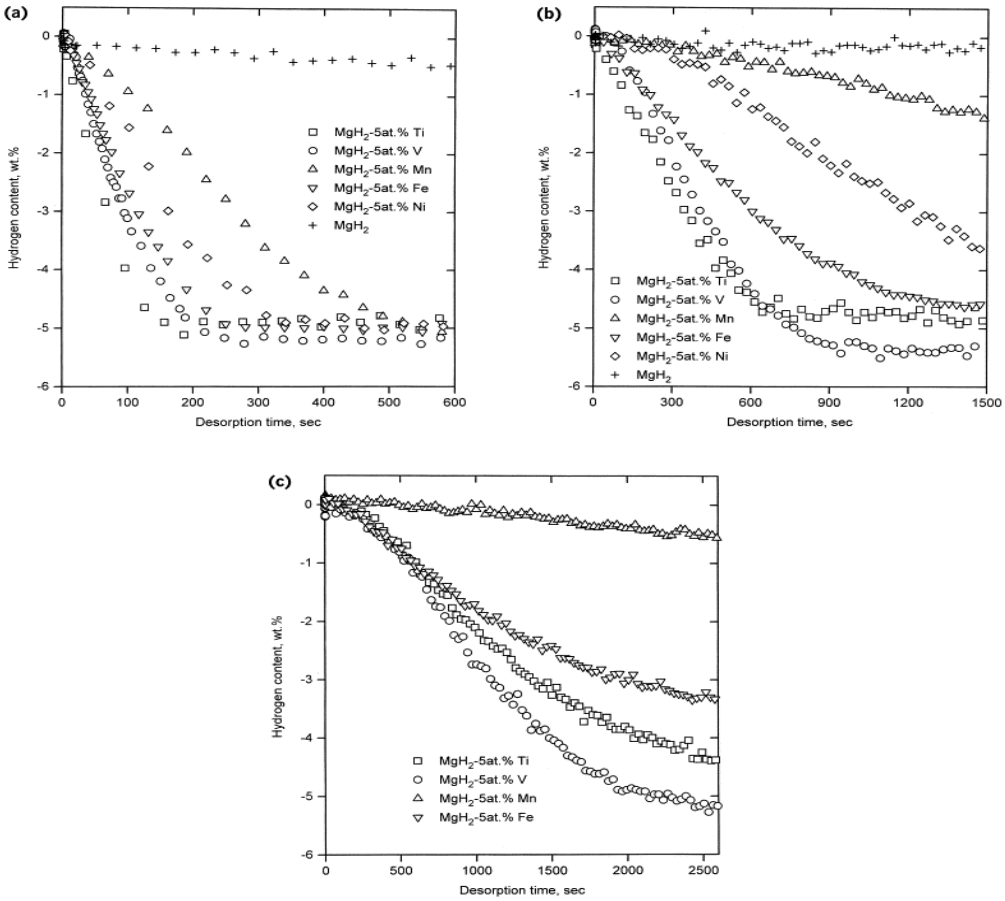

Figure 5. Desorption curves of MgH_2-5 at%Tm (Tm = Ti, V, Mn, Fe and Ni) composites under a hydrogen pressure of 0.015MPa at: (**a**) 573 K; (**b**) 523 K; (**c**) 508 K. (Copyright Elsevier 1999 [17].)

In another study, Rizo-Acosta et al. performed a comparative study of early transition metal doped (Sc, Y, Ti, Zr, V, and Nb) MgH_2 and found that Y and V allowed for the highest absorption performances. The sequence of hydrogen absorption was Y < V < Ti < Nb < Sc < Zr. Nevertheless, with an increasing number of cycles, a slight degradation was observed but this effect was less evident for the Ti doped system, which revealed better hydrogenation properties in terms of cycling and wt% [47]. All of the studies indicate that the Ti-based additives or catalysts play a crucial role in the improvement of the hydrogenation properties of MgH_2.

3.2. Titanium-Based Additives

Effects of various Ti-based additives or catalyst such as Ti hydride, halide and oxide have been studied. Researchers observed a dramatic improvement in the hydrogen kinetics by addition of Ti [48–51].

3.2.1. Titanium or Titanium Hydride

Choi et al. observed that MgH_2-TiH_2 shows significant enhancement in the kinetics compared to pure MgH_2 ball milled at the same conditions, with onset of the desorption temperature at 400 K at a heating rate of 5 K/min [52].

Kinetic energy of ball milled MgH_2 is 96 kJ/mol and after adding TiH_2 the kinetic energy is reduced by 15 kJ/mol. This shows the positive effect of TiH_2 on hydrogen storage of MgH_2. Desorption enthalpy also reduces in a MgH_2-TiH_2 sample by the effect of TiH_2. According to experimental results, the dehydrogenation properties of the MgH_2 can be improved by TiH_2 addition, which also weakens the Mg−H bond [53]. These findings encourage additional research into how TiH_2 affects the hydrogen absorption

and desorption capabilities of MgH_2 [54,55]. N. Patelli et al. [56] synthesised Mg-Ti-H nanoparticles with different Ti contents, from 14 to 63 at%, by gas phase condensation and investigated the sorption kinetics in the temperature range 100–150 °C. Results reveal an increase of the activation energy with Ti content in the range 43−52 kJ/mol and an increase of the rate constant (at 150 °C) from $27\times10\ s^{-1}$ to $92\times10\ s^{-1}$. Choi et al. [57] studied the hydrogenation properties of Ti-added MgH_2 composite (MgH_2 + 15 Ti). They observed that Ti enhances the kinetics of MgH_2. Samples absorbed 2.96 wt% H in 2.5 min and 5.51 wt% H in 60 min at 593. K.M. Lototskyy [58] observed that the introduction of a small amount of graphite improves the hydrogen storage performance of MgH_2. In Table 2, the hydrogen storage properties of Mg/MgH_2 with elemental Ti or TiH_2 additive for different authors are reported.

Table 2. Hydrogen storage properties of Mg/MgH_2 with elemental Ti or TiH_2 additive.

Materials	Synthetic Method	T_{des}	Hydrogen Desorption Capacity (wt%)	Activation Energy (kJ/mol H_2)	Reference
$7MgH_2/TiH_2$	Ball milling	126 °C	5.5	79	[53]
$10MgH_2/TiH_2$	Ball milling	101 °C	5	71	[53]
MgH_2-1 at%Ti	Ball milling	278 °C	4.9	208	[49]
MgH_2-5 at%Ti	Ball milling	274 °C	4.5	156	[49]
MgH_2-Ni/Ti	Ball milling	256 °C	2.9	81	[49]
MgH_2-$Ti_5Fe_5Ni_5$	Ball milling	270 °C	5.3	45.63	[50]
MgH_2-Ti_2	Ball milling	257 °C	6.18	103.9	[51]
MgH_2-0.1TiH_2	Ultrahigh-energy−high pressure (UHEHP) ball milling	290 °C	6.20	58.4	[54]
0.7MgH_2–0.3TiH_2	Reactive ball milling	573 K less than 100 s	-		[59]
$MgH_2/0.1TiH_2$	High pressure ball milling	269–301	-	77.4	[60]
Mg-2% Ti	Inert gas condensation	320 °C	4.50		[61]
MgH_2 + 2 at%Ti	Cold rolling (5 times, air)	623 K	6.00		[62]
MgH_2-4 mol%Ti	Ball Milling	573 K	1.10		[63]
MgH_2-5 at%Ti	Ball Milling	235.6 °C		70.11	[64]
MgH_2-5 at%Ti	Ball Milling	523 K	5.50	71.1	[64]
MgH_2-5 at%Ti		573 K	5.20		[64]
Mg-5%Ti	Chemical Vapor Synthesis			104	[65]
Mg-14 at%Ti	Gas phase condensation			35	[56]
MgH_2-15%Ti	Ball Milling	573 K	0.12		[57]
$Mg_{0.9}Ti_{0.1}$	Ball Milling			76	[58]
$Mg_{0.75}Ti_{0.25}$	Ball Milling			88	[58]
$Mg_{0.5}Ti_{0.5}$	Ball Milling			91	[58]
MgH_2-20%Ti	Ball Milling			72 ± 3	[66]
MgH_2-coated Ti	Ball Milling	250 °C	5.00		[66]
$Mg_{83.5}Ti_{16.5}$	Ball Milling	300 °C	2.50		[67]
15Mg-Ti	Chemical Method				[68]
MgH_2-5 at%Ti	Chemical Method	270 °C	5.80	67.24	[63]
$4MgH_2$-TiH_2	Ball Milling			68	[52]
MgH_2 + 10 mol%TiH_2	Ball Milling			16.24	[55]
Mg-9.2% $TiH_{1.971}$-3.7%$TiH_{1.5}$	Ball Milling	573 K	4.10	46.2	[69]
$Mg_{0.65}Ti_{0.35}D_{1.2}$	Ball Milling			17	[70]

3.2.2. Titanium Oxide

Metal oxides have a catalytic effect as well as they act as a milling aid by creating defects in the MgH_2 structure. Among various used catalysts, TiO_2 cost is low, it presents large availability with respect to other oxides and it consists of numerous interesting catalytic characteristics [71–74]. M. Polanski et al. [72] investigated the effect of several oxides (Cr_2O_3, TiO_2, Fe_3O_4, Fe_2O_3, In_2O_3 and ZnO) on ball-milled MgH_2. Experimental results reveal that Cr_2O_3 and TiO_2 are superior catalysts because they enhance MgH_2 absorption and desorption properties. S. K. Pandey et al. [75] observed that particles of 50 nm diameter allowed for the lowest activation energy, confirming that particle size of TiO_2 is an important factor in the sorption properties of magnesium hydride. Further, M. Daryani et al. [76] investigated that, by the addition of Ti-based catalysts, the activation energy of MgH_2 is reduced by up to 20–30 kJ/mol. They also observed a significant improvement in desorp-

tion kinetics during cyclic dehydrogenation of MgH_2 due to the presence of micro-cracks at the particle surfaces. D. Mirabile Gattia et al. synthesised MgH_2-5%TiO_2-5%ENG pellets by ball milling followed by cold pressing at various compaction loads. The pellets fabricated at the highest pressure showed improved performance [77,78]. Y. C. Pan et al. [42] prepared the Mg-TiO_2 composite by the arc plasma method and found that TiO_2 can act as a catalyst to improve the hydrogenation properties of Mg. K.S. Jung et al. [79] and R. Vujasin et al. [80] studied the effect of different phases of TiO_2, such as anatase and rutile, on the sorption properties of magnesium hydride. X. Zhang et al. [80] studied the effect of carbon-supported nanocrystalline TiO_2 (TiO_2@C) on the hydrogenation properties of MgH_2 and found that MgH_2-10 wt%TiO_2@C started to desorb and absorb hydrogen at 205 °C and room temperature, respectively, revealing the catalytic activity of carbon-supported nanocrystalline TiO_2. Mg-5 mol% $Ti_4Fe_2O_x$ also absorbs hydrogen at room temperature after desorption and after the addition of 3 wt% graphite the cyclic stability was sustained, as reported by V. Berezovets et al. [81]. In Table 3, the hydrogen sorption properties of MgH_2 and titanium oxides are reported.

Table 3. Hydrogen storage properties of Mg/MgH_2 with elemental Ti or TiO_2 additive.

Materials	Synthetic Method	$T_{des.}$	Hydrogen Desorption Capacity (wt%)	E_{act}(kJ/mol H_2)	Reference
Mg-TiO_2	Arc evaporation	300 °C	6.34	77.2	[42]
MgH_2-5 mol%TiO_2 (rutile)	Ball milling	300 °C	4.40		[78]
MgH_2-5 mol%TiO_2 (anatase)	Ball milling	300 °C	1.95	52.7	[78]
MgH_2-10% TiO_2	Ball Milling	300 °C	6.00		[82]
MgH_2-20% TiO_2	Ball Milling	350 °C	4.40		[83]
MgH_2 +5 wt%TiO_2(np) (>50 nm)	Ball Milling	335 °C			[75]
MgH_2 + 5 wt%TiO_2 (np) (<50 nm)	Ball milling	310 °C		57	[75]
MgH_2 + 6% TiO_2	Ball Milling			145.8	[84]
MgH_2 +10% TiO_2	Ball Milling	200 °C		75.50	[85]
MgH_2-x wt%TiO_2@C	Ball Milling	195 °C	6.2	106	[79]
MgH_2-TiO_2@rGO-EA	Ball Milling	265 °C	4.2	86.7 ± 8.0	[86]
MgH_2-40TiO_2@rGO-EG	Ball Milling	261 °C	5.9		[86]

3.2.3. Titanium Halide

S.-A. Jin et al. [87] performed a comparative study of the effect of VF_4, NbF_5, NiF_2, TiF_3, CrF_2, CuF_2, FeF_2, ZrF_2 and YF_3 on the hydrogenation properties of MgH_2 and observed that, among various transition metal fluorides, NbF_5 and TiF_3 showed a better catalytic effect. The formation of a MgF_2 layer has been observed, due to the reaction of MgH_2 with metal halides during the process of milling and releasing of hydrogen. Moreover, MgF_2 contains an F^- anion having a high affinity towards hydrogen and weakening the Mg−H bonding [88–93]. In another study S.-A. Jin et al. reported that, when MgH_2 reacts with TiF_3, the formation of TiH_2 also takes place, following the formula: $3MgH_2 + 2\ TiF_3 \rightarrow 3MgF_2 + 2TiH_2 + H_2$.

Further remarkable effect of magnesium fluoride has been reported by I.E. Malka et al. [93]. MgF_2 acts as a catalyst and it enhances the sorption kinetics of MgH_2. Halides having the highest oxidation state reduce the magnesium decomposition temperature more efficiently than their counterparts with a lower oxidation state [93]. Study of the effect of various halide additives reveals that fluorides are better catalysts than chlorides. S.-K. Peng et al. [94] investigated the hydrogenation properties of TiF_3 and TiF_4 doped Mg$(AlH_4)_2$ and they observed that TiF_4 shows superior catalytic abilities due to the higher oxidation state of Ti. M. Jangir et al. [95] studied the effect of TiF_4 on MgH_2 and found that hydrogen properties of MgH_2 markedly improved by TiF_4 addition by lowering the onset desorption temperature compared to as-milled MgH_2. In Table 4, the sorption properties of MgH_2 with different halides for different authors are reported.

Table 4. Hydrogen sorption properties for Mg-based compounds with halides.

Materials	Synthetic Method	$T_{des.}$	Hydrogen Desorption Capacity (wt%)	E_{act} (kJ/mol H_2)	Reference
MgH_2 + 4 mol%TiF_3	Ball milling	173 °C	6.14		[51]
MgH_2 + 4 mol%TiF_3	Ball milling	300 °C	5		[96]
MgH_2 + 5 wt%TiF_3	Ball milling	300 °C	5.5		[97]
MgH_2 + 10 wt%K_2TiF_6	Ball Milling	245 °C	6.5		[98]
MgH_2 + 7 wt%$TiCl_3$	Ball Milling	225 °C		79	[93]
MgH_2-10% TiF_4	Ball Milling	216 °C	6.6	71	[99]
MgH_2-10% TiF_4	Ball milling	154 °C		70	[95]
MgH_2 + 4 mol%TiF_3	Ball Milling	573 °C	4.5		[63]
MgH_2 + 4 mol%$TiCl_3$	Ball Milling	573 °C		3.70	[63]

Furthermore, a comparative study of various Ti-based additive such as elemental Ti, TiO_2, TiN and TiF_3 has been carried out by Y. Wang et al. [51]. Different Ti-based materials are added to MgH_2 and their catalytic effects are studied thoroughly. The findings revealed that all of these Ti-based compounds may significantly increase MgH_2 dehydrogenation performance. TiF_3 has the best catalytic properties, followed by elemental Ti, oxide TiO_2 and covalent TiN in that order.

The initial desorption temperature drops from 308 °C for pure MgH_2 to 280 °C for MgH_2-TiN, then to 257 and 216 °C for MgH_2-Ti and MgH_2-TiO_2 composites and ultimately to 173 °C for the MgH_2-TiF_3 sample. The reduced E_a also indicated the favourable impacts of these additives, which were 10.3%, 26.3%, 35.8% and 53.3% lower following the addition of TiN, TiO_2, Ti and TiF_3, respectively. Mechanism analyses revealed that the covalent TiN was stable throughout the dehydrogenation process. During ball milling, elemental Ti and ionic TiF_3 react with MgH_2 to create active $TiH_{1.971}$ and TiH_2, which operate as active species throughout the desorption. The degradation of the MgH_2-TiO_2 sample occurred in two steps. As a result, the diverse reaction mechanisms and active species can explain the various effects of these Ti-based materials on the dehydrogenation capabilities of MgH_2 [95].

3.2.4. Ti-Based Intermetallics

In recent years Ti-based intermetallics as catalysts have captivated the interest of researchers. TiFe [100–102], $(Fe_{0.8}Mn_{0.2})Ti$ [103], Ti_2Ni [104] and $TiMn_{1.5}$ [105] additives showed good catalytic effects in improving the hydrogen storage properties of MgH_2. C. Zhou et al. [64] investigated the effect of a series of intermetallic additives (i.e., TiAl, Ti_3Al, TiNi, TiFe, TiNb, $TiMn_2$ and TiVMn) and observed that $TiMn_2$-doped Mg was capable of absorbing hydrogen at room temperature. They also reported that the apparent activation energy is 20.59 kJ/mol·H_2. These results have been confirmed by El-Eskandarany et al. [106,107] and also by the first principles calculation performed by J.H. Dai et al. [108]. V.V. Berezovets et. al. investigated the hydrogen absorption and desorption capabilities of nanostructured MgH_2 modified with Ti-based materials (nano-Ti, nano-TiO_2 and $Ti_4Fe_2O_x$) and produced by reactive ball milling in hydrogen. In the case of nano-Ti and $Ti_4Fe_2O_x$ additions, a greater hydrogen storage capacity was attained [81]. In Table 5 hydrogen sorption properties of Mg-based compounds with Ti intermetallics and alloys are reported.

Table 5. Hydrogen sorption properties of Mg-based compounds with Ti intermetallics and alloys.

Materials	Synthetic Method	$T_{des.}$	Hydrogen Desorption Capacity (wt%)	E_{act} (kJ/mol H_2)	Reference
MgH_2-5 at%TiAl	Ball milling	270 °C	4.90	65.08	[64]
MgH_2-5 at%Ti_3Al	Ball milling	232.3		70.61	[64]
$Mg_{85}Al_{7.5}Ti_{7.5}$	DC-Magnetron Co-Sputtering	200 °C	5.30		[109]
$Mg_{0.63}Ti_{0.27}Si_{0.10}D_{1.1}$	Ball Milling			27	[70]
MgH_2-5 at%TiNi	Ball Milling	242.4 °C		73.09	[64]
15Mg-Ti-0.75Ni	Chemical method			63	[68]
MgH_2-5 at%TiNb	Ball Milling	27 °C	5.90	71.72	[64]
MgH_2-5 at%Cr-5 at%Ti	Film	200 °C	6.00	3.70	[110]
MgH_2-7 at%Cr-13 at%Ti	Film	200 °C	5.00		[110]
MgH_2-5 at%TiFe	Ball Milling	270 °C	5.20	72.63	[64]
MgH_2-5 at%$TiMn_2$	Ball Milling	270 °C	4.60	74.22	[64]
$Mg_{87.5}Ti_{9.6}V_{2.9}$	Hydrogen plasma metal reaction	300 °C	4.00	73.08	[69]
MgH_2-5 at%TiVMn	Ball Milling	270 °C	5.70	85.20	[64]

3.2.5. Titanium Carbides and Carbonitrides

MXene is a newly developed, two-dimensional transition metal carbide or carbonitride and is structurally comparable to graphene. One of the oldest and most extensively used MXenes for improving the hydrogen storage properties of MgH_2 is Ti_3C_2 [111]. The 2D Ti_2C MXene has a good catalytic impact on MgH_2 dehydrogenation. MgH_2-5 wt%Ti_2C has a lower onset dehydrogenation temperature, reduced to 37 °C, the apparent activation energy, E_a, is 36.5% lower and the total enthalpy changes (ΔH) are higher than those of pure MgH_2 (11%) [112]. Further, Y. Liu et al. used ball milling to incorporate a two-dimensional $Nb_4C_3T_x$ (MXene) produced through chemical exfoliation into MgH_2. The activated MgH_2-5 wt%$Nb_4C_3T_x$ composite has excellent hydrogen storage kinetics [113]. According to the findings, the use of a novel two-dimensional Ti_3C_2 MXene-based catalyst (Ni@Ti-MX) improved the MgH_2 hydrogen sorption significantly [114].

Microstructural investigations demonstrated that the as-prepared Ni@TiMX, which has a uniform dispersion of self-assembled Ni nanoparticles on its surface, reacts with MgH_2 during de/hydrogenation cycles, resulting in the creation of multiphase components (Mg_2Ni, TiO_2, metallic Ti or amorphous C) [115].

W. Zhu et al. demonstrated a method for using delaminated Ti_3C_2 folded nanosheets (MXenes) as a support material for nanoconfinement of MgH_2/Mg NPs with a high loading capacity. Microstructural and property tests demonstrated that the Ti-MX support material not only acted as a scaffold to anchor the ultradispersed MgH_2/Mg NPs (15 nm), but also had a substantial catalytic effect in increasing the hydrogen storage performances of MgH_2 NPs without the use of a doping catalyst [116].

By alkali treating Ti_3C_2 MXene, an unusual Hamamelis-like structure of $K_2Ti_6O_{13}$, with branches 1020 nm in length, is synthesised. It has an excellent catalytic activity for hydrogen desorption from MgH_2 [117]. Y. Wang studied the investigated the remarkable enhancing impact of PrF_3 on Ti_3C_2 MXene using a hydrothermal technique, and it demonstrated a superior catalytic effect on hydrogen storage in MgH_2 [118].

Sheng et al. [119] attempt to use $(Ti_{0.5}V_{0.5})_3C_2$ to lower the initial temperature of the hydrogen desorption of MgH_2 to 210 °C. It was demonstrated that MgH_2 reacted with $(Ti_{0.5}V_{0.5})_3C_2$ to form Ti and V metals, which were suggested to act as active catalysts for the hydrogen sorption process.

In order to create a sandwich-like Ti_3C_2/TiO_2, Gao et al. [120] partially oxidised Ti_3C_2 MXene. At a constant temperature of 250 °C, the MgH_2 + 5 wt% of Ti_3C_2/TiO_2 can desorb 5.0 wt% of hydrogen while it absorbs 4.0 wt% at a temperature of 125 °C. The enhancement

of MgH_2 by Ti_3C_2/TiO_2 was thought to be caused by the layered structures and the various valence Ti-containing compounds.

By exfoliating V_2AlC and Ti_3AlC_2, Liu et al. [121] created V_2C and Ti_3C_2 MXenes. At about 180 °C, MgH_2 +10 wt% of $2V_2C/Ti_3C_2$ started the hydrogen desorption process, and after 60 min at 225 °C, 5.1 wt% of the hydrogen was desorbed. During the desorption process, hydrogen atoms or molecules may transfer preferentially through the $MgH_2/V_2C/Ti_3C/Ti_3C_2$ triple-grain boundaries, and during the absorption process, through the Mg/Ti_3C_2 interfaces. Specifically, V_2C and Ti_3C_2 simultaneously function as effective catalysts for MgH_2. Chen et al. [122] added Ti_3C_2 to a $4MgH_2$-$LiAlH_4$ composite; the dehydrogenation onset temperature of the $4MgH_2$-$LiAlH_4$-Ti_3C_2 composite was reduced by 64 K and 274 K, respectively, with $4MgH_2$-$LiAlH_4$ and as-milled MgH_2. The Ti produced in situ from the MXene Ti_3C_2 is responsible for the destabilisation of $4MgH_2$-$LiAlH_4$. Few-layer Ti_3C_2 can only exist in solution as a film and is easily agglomerated, reducing the number of active hydrogen absorption and desorption sites. Multilayer Ti_3C_2 (ML-Ti_3C_2), on the other hand, can exist as a solid powder, making it easier to form a composite with MgH_2. According to the experimental findings, the initial desorption temperature of MgH_2-6 wt% ML-Ti_3C_2 is lowered to 142 °C with a 6.56 wt% capacity. In the MgH_2-6 wt% ML-Ti_3C_2 hydrogen storage system, the E_a of hydrogen desorption is around 99 kJ/mol, which is 35.3% less than that of pure MgH_2. Two complementary effects, one in which Ti facilitates the easier dissociation or recombination of hydrogen molecules and the other in which multivalent Ti generates electron transfer that facilitates the simpler conversion of hydrogen, are responsible for the enhancement of kinetics in hydrogen absorption and desorption by ML-Ti_3C_2 [120].

X. Huang et al. [123] studied the effect of Ti_3CN MXene on the hydrogenation properties of MgH_2. They observed that Ti_3CN MXene lowers the operating temperature and improves the kinetics of MgH_2. Desorption enthalpy changes for MgH_2 and MgH_2 + 7.5 wt%Ti_3CN were 79.3 and 78.8 kJ mol^{-1}, respectively. Using Ti_3CN does not affect the MgH_2's thermal stability.

El-Eskandarany et. al. ball milled MgH_2 with titanium carbide and studied its sorption properties at 275 °C under a hydrogen gas pressure in the range 100 mbar to 8 bar [124]. R.M.A. Khalil et al. performed an ab initio study on the properties of MgH_2 and TiC systems [125].

Z. Tian et al. synthesised transition metal carbides (Ti_3C_2, Ni_3C, Mo_2C, Cr_3C_2 and NbC) to improve the hydrogen storage behaviours of magnesium-based materials. Mechanical ball milling was used to incorporate carbides with a weight ratio of 5% into MgH_2, and the microstructure, phase composition and hydrogen storage capabilities of the composites were thoroughly investigated. All of these metal carbides can improve the MgH_2's hydrogen absorption and desorption kinetics. Ti_3C_2 demonstrated the best catalytic effect on MgH_2 dehydrogenation kinetic characteristics, followed by Ni_3C, NbC, Mo_2C and Cr [126].

3.3. Other Catalysts and Additives

In this section, some recent developments on catalysts for MgH_2 are reported, which consider different approaches based on the use of perovskites, ternary metal oxides, metal alloys and core-shell particles.

Hydrogen storage performance can be improved when cobalt lanthanum oxide ($LaCoO_3$) is added via the ball milling process. When compared to pure MgH_2 and milled MgH_2, the results demonstrate that adding 10 weight per cent $LaCoO_3$ significantly reduces the beginning hydrogen release. However, when compared to milled MgH_2 under the same conditions, quicker ab/desorption was seen with the addition of 10 weight per cent $LaCoO_3$. Additionally, when compared to milled MgH_2, the apparent activation energy for MgH_2-10 wt% $LaCoO_3$ was significantly lower [127].

X. Yang et al. [128] proved that adding cubic K_2MoO_4 to magnesium hydride could change its kinetic characteristics. Its distinctive cubic structure produces novel species during the absorption and desorption of hydrogen, and this produces exceptional catalytic

activity during the storage of hydrogen in MgH_2. The quantity of K_2MoO_4 affects the duration of hydrogen dissociation and adsorption. The kinetic performance is faster and the time used is shorter with an increasing amount of K_2MoO_4. Studies on the catalytic process reveal that K_2MoO_4 is evenly spread across the MgH_2 substrate's surface. The reaction resulted in the formation of three new compounds, KH, MgO and $MgMo_2O_7$, which collectively enhanced the hydrogen storage capabilities of MgH_2. They increase the number of catalytically active sites, which increases the speed of the hydrogenation processes and shortens the hydrogen pathways, which lowers the energy barriers for H dissociation and absorption.

M.S. El-Eskandarany et al. [129] observed that the dehydrogenation kinetics of the Zr_2Ni-milled samples were promising, as indicated by the short time (700 s) required to release their full storage capacity (6.2 wt%H_2). The powders also demonstrated remarkable cyclability, as it was possible to reach 646 cycles in 985.5 h without experiencing significant deterioration.

The exact impacts of the Ni@C material addition on the hydrogen desorption properties of the MgH_2-x wt% Ni@C (x = 0, 1, 2, 4 and 6) composites have been discussed by the C. An et al. According to the experimental results, MgH_2-Ni@C composites' dehydrogenation kinetics can be positively improved by the addition of Ni@C components [130].

4. Discussion

The discovery and identification of suitable catalysts is critical for the development of Mg-based hydrogen storage systems. Numerous attempts at catalyst optimisation have resulted in significant improvements in the hydrogen absorption/desorption kinetics of MgH_2. The multivalence transition metals as well as their oxides, hydrides, halides, carbides and carbonitrides and intermetallics have been shown to outperform other additions in catalysis.

Transition metal-based additions showed improved hydrogen storage characteristics of MgH_2. Ti and its compounds are recognised as a potential group of transition metal-based additives that have been extensively researched in many various aspects, including catalytic effects, catalysis mechanism, nano- and microstructures and synthesis methods. This group of additives has received a lot of attention and effort over the last few decades, and progress has been made. We seek to present overviews of specific fundamental concepts and clear catalytic mechanisms for Mg-based materials, with a special emphasis on Ti-based catalysts.

Furthermore, the hydrogen storage properties of the MgH_2-TiF_3 composite outperform those of the MgH_2-TiH_2 composite. As the Ti species is introduced into magnesium, TiF_3 aids in the dissociation of the hydrogen molecule at low temperatures. A study of TiF_3 and $TiCl_3$ additives revealed that TiF_3 had a superior catalytic effect to $TiCl_3$. This result revealed that the F^- anion has a particular catalytic role. It was discovered that titanium chloride and fluoride reacted similarly with MgH_2 during milling or hydrogen cycling operations, creating TiH_2 and $MgCl_2$ or MgF_2. As a result, it was believed that the fluoride anion would produce catalytically active species, but the chloride anion would not.

Although a complete knowledge of the role of Ti-based catalysts is still lacking, evidence suggests that catalysts do play key roles in encouraging certain of the processes. The doped catalyst species might lower the hydrogen molecule's dissociation energy barrier while simultaneously facilitating hydrogen transport in the Mg/MgH_2 matrix. Kinetic modelling could become a more valuable tool for interpreting reaction control processes. Future mechanism research should focus on observing catalytic activity and microstructure evolution under carefully regulated reaction circumstances in order to give more accurate comparisons with boundary conditions for the different models used for interpretation.

5. Future Prospects and Challenges

Storage of hydrogen in safe and operable conditions remains a key challenge. Current literature proposes extensive possibilities of storing hydrogen in metal hydrides, however, to achieve suitable hydrogen absorption/desorption kinetics at ambient conditions, further

rigorous research would be required. Various catalysts or additives have been studied to enhance the hydrogen absorption/desorption kinetics in solid hydrogen storage materials. Catalysts significantly improve the hydrogen sorption kinetics in metal hydride, providing fast and effective dissociation of hydrogen molecules. The addition of the additive to MgH_2 reduced the activation energy for dehydrogenation, therefore, lowering the decomposition temperature and improving the desorption properties of MgH_2. However, it is still difficult to assess the effectiveness of different catalysts. The mechanism of catalysis consists of several steps. For example, in the process of hydrogenation, these steps include hydrogen dissociation, surface penetration, diffusion, hydride nucleation and growth. In spite of many efforts by researchers to understand the role of the catalyst in improving the kinetics of solid-state hydrogen storage materials, some aspects remain unclear. Several findings suggested that the use of an additive or of a catalyst can reduce the dissociation energy barrier of the hydrogen molecule, and it can promote the hydrogen diffusion in the Mg/MgH_2 matrix. Interpreting the controlling steps of the reactions kinetic modelling could become a crucial tool. Future mechanism studies should look on the development of the microstructure and catalytic activity under tightly controlled reaction conditions. Moreover, the development of effective catalysts for hydrogen storage at the solid state requires further research. As reviewed in this work, among the different types of catalysts, Ti-based additive was revealed to be highly effective in enhancing the hydrogen properties of MgH_2. Effect of various types of Ti-based catalysts including hydrides, oxides, halides, carbides, carbonitrides and intermetallics on the dehydrogenation and hydrogenation kinetics have been studied by researchers in the last few decades. These promising results could be at the base of suitable hydrogen storage systems in view of a future hydrogen-based economy.

Author Contributions: M.J., I.P.J. and D.M.G. contributed in the same manner to the manuscript. All authors have read and agreed to the published version of the manuscript.

Funding: This research received no external funding.

Data Availability Statement: No new data were created or analyzed in this study. Data sharing is not applicable to this article.

Conflicts of Interest: The authors declare no conflict of interest.

References

1. Pérez-Lombard, L.; Ortiz, J.; Pout, C. A review on buildings energy consumption information. Energy Build. *Energy Build.* **2008**, *40*, 394–398. [CrossRef]
2. Schlapbach, L.; Zuttel, A. Hydrogen storage materials for mobile applications. *Nature* **2001**, *414*, 353–358. [CrossRef]
3. Dincer, I. Renewable energy and sustainable development: A crucial review. *Renew. Sust. Energ. Rev.* **2000**, *4*, 157–175. [CrossRef]
4. Sakintuna, B.; Lamari-Darkrim, F.; Hirscher, M. Metal hydride materials for solid hydrogenstorage: A review. *Int. J. Hydrog. Energy* **2007**, *32*, 1121–1140. [CrossRef]
5. Principi, G.; Agresti, F.; Maddalena, A.; Russo, S.L. The problem of solid state hydrogenstorage. *Energy* **2009**, *34*, 2087–2091. [CrossRef]
6. Berube, V.; Radtke, G.; Dresselhaus, M.; Chen, G. Size effects on the hydrogen storage properties of nanostructured metal hydrides: A review. *Int. J. Energy Res.* **2007**, *31*, 637–663. [CrossRef]
7. Huot, J.; Liang, G.; Boily, S.; Van Neste, A.; Schulz, R.J. Structural study and hydrogen sorption kinetics of ball-milled magnesium hydride. *J. Alloys Compd.* **1999**, *293*, 495–500. [CrossRef]
8. Zaluska, A.; Zaluski, L.; Strom-Olsen, J.O.J. Nanocrystalline magnesium for hydrogen storage. *J. Alloys Compd.* **1999**, *288*, 217–225. [CrossRef]
9. Wagemans, R.W.P.; Lenth, J.H.V.; de Jongh, P.E.; Dillen, A.J.V.; de Jong, K.P. Hydrogen storage in magnesium clusters: Quantum chemical study. *J. Am. Chem. Soc.* **2005**, *127*, 16675–16680. [CrossRef]
10. Zhang, Q.; Zang, L.; Huang, Y.; Gao, P.; Jiao, L.; Yuan, H.; Wang, Y. Improved hydrogen storage properties of MgH_2 with Ni-based compounds. *Int. J. Hydrog. Energy* **2017**, *42*, 24247–24255. [CrossRef]
11. Zhang, J.; Li, Z.; Wu, Y.; Guo, X.; Ye, J.; Yuan, B.; Wang, S.; Jiang, L. Recent advances on the thermal destabilization of Mg-based hydrogen storage materials. *RSC Adv.* **2019**, *9*, 408–428. [CrossRef] [PubMed]
12. Dornheim, M.; Doppiu, S.; Barkhordarian, G.; Boesenberg, U.; Klassen, T.; Gutfleisch, O. Hydrogen storage in magnesium-based hydrides and hydride composites. *Scr. Mater.* **2007**, *56*, 841–846. [CrossRef]

13. Webb, C.J. A review of catalyst-enhanced magnesium hydride as a hydrogen storage material. *J. Phys. Chem. Solid.* **2015**, *85*, 96–106. [CrossRef]
14. Li, J.; Li, B.; Shao, H.; Li, W.; Lin, H. Catalysis and downsizing in Mg-based hydrogen storage materials. *Catalysts* **2018**, *8*, 89. [CrossRef]
15. Xie, X.; Chen, M.; Hu, M.; Wang, B.; Yu, R.; Liu, T. Recent advances in magnesium-based hydrogen storage materials with multiple catalysts. *Int. J. Hydrog. Energy* **2019**, *44*, 10694–10712. [CrossRef]
16. Danaie, M.; Tao, S.X.; Kalisvaart, P.; Mitlin, D. Analysis of deformation twins and the partially dehydrogenated microstructure in nanocrystalline magnesium hydride (MgH_2) powder. *Acta Mater.* **2010**, *58*, 3162–3172. [CrossRef]
17. Liang, G.; Huot, J.; Boily, S.; Van Neste, A.; Schulz, R. Catalytic effect of transition metals on hydrogen sorption in nanocrystalline ball milled MgH_2-Tm (Tm = Ti, V, Mn, Fe and Ni) systems. *J. Alloys Compd.* **1999**, *292*, 247–252. [CrossRef]
18. Hanada, N.; Ichikawa, T.; Fujii, H. Catalytic effect of nanoparticle 3d- transition metals on hydrogen storage properties in magnesium hydride MgH_2 prepared by mechanical milling. *J. Phys. Chem. B* **2005**, *109*, 7188–7194. [CrossRef]
19. Mohsen, D.; Cesario Asselli, A.A.; Huot, J.; Botteon, G.A. Formation of the ternary complex hydride Mg_2FeH_6 from magnesium hydride (β-MgH_2) and Iron: An electron microscopy and energy-loss spectroscopy study. *J. Phys. Chem. C* **2012**, *116*, 25701–25714.
20. Tan, Z.; Chun, C.; Heilweil, E.J.; Bendersky, L.A. Thermodynamics, kinetics and microstructural evolution during hydrogenation of iron- doped magnesium thin films. *Int. J. Hydrog. Energy* **2011**, *36*, 9702–9713. [CrossRef]
21. Zahiri, B.; Harrower, C.T.; Amirkhiz, B.S.; Mitlin, D. Rapid and reversible hydrogen sorption in Mg-FeTi thin films. *Appl. Phys. Lett.* **2009**, *95*, 103114. [CrossRef]
22. Gasan, H.; Celik, O.N.; Aydinbeyli, N.; Yaman, Y.M. Effect of V, Nb, Ti graphite addition on the hydrogen desorption temperature of magnesium hydride. *Int. J. Hydrog. Energy* **2012**, *37*, 1912–1918. [CrossRef]
23. Sohn, H.Y.; Emami, S. Kinetics of dehydrogenation of the Mg-Ti-H hydrogen storage system. *Int. J. Hydrog. Energy* **2011**, *36*, 8344–8350. [CrossRef]
24. Stampfer, J.F.; Holley, C.E.; Suttle, J.F. The Magnesium-hydrogen system. *J. Am. Chem. Soc.* **1960**, *82*, 3504–3508. [CrossRef]
25. Bastide, J.P.; Bonnetot, B.; Letoffe, J.M.; Claudy, P. Polymorphisme de l'hydrure de magnesium sous haute pression. *Mater. Res. Bull.* **1980**, *15*, 1215–1224. [CrossRef]
26. Bortz, M.; Bertheville, B.; Bottger, G.; Yvon, K. Structure of the high pressure phase γ-MgH_2 by neutron powder diffraction. *J. Alloys Compd.* **1999**, *287*, L4–L6. [CrossRef]
27. Magnesium-hydride-unit-cell-3D-balls. Available online: https://commons.wikimedia.org/wiki/File:Magnesium-hydride-unit-cell-3D-balls.png (accessed on 8 August 2022).
28. Vajeeston, P.; Ravindran, P.; Hauback, B.C.; Fjellvåg, H.; Kjekshus, A.; Furuseth, S.; Hanfland, M. Structural stability and pressure-induced phase transitions in MgH_2. *Phys. Rev. B* **2006**, *73*, 224102. [CrossRef]
29. Dornheim, M. Thermodynamics of Metal Hydrides: Tailoring Reaction Enthalpies of Hydrogen Storage Materials. In *Thermodynamics-Interaction Studies-Solids, Liquids and Gases*; IntechOpen: London, UK, 2011. [CrossRef]
30. Satyapal, S.; Petrovic, J.; Read, C.; Thomas, G.; Ordaz, G. The U.S. Department of Energy's National Hydrogen Storage Project: Progress towards meeting hydrogen-powered vehicle requirements. *Catal. Today* **2007**, *120*, 246–256. [CrossRef]
31. Kohno, T.; Tsuruta, S.; Kanda, M. The hydrogen storage properties of new Mg2Ni alloy. *J. Electrochem. Soc.* **1996**, *143*, 198–199. [CrossRef]
32. Shao, H.; Wang, Y.; Xu, H.; Li, X. Preparation and hydrogen storage properties of nanostructured Mg2Cu alloy. *J. Solid. State Chem.* **2005**, *178*, 2211–2217. [CrossRef]
33. Bououdina, M.; Guo, Z.X. Comparative study of mechanical alloying of (Mg+ Al) and (Mg+ Al+ Ni) mixtures for hydrogen storage. *J. Alloys Compd.* **2002**, *336*, 222–231. [CrossRef]
34. Chaudhary, A.-L.; Sheppard, D.A.; Paskevicius, M.; Webb, C.J.; Gray, E.M.; Buckley, C.E. Mg_2Si Nanoparticle Synthesis for High Pressure Hydrogenation. *J. Phys. Chem. C* **2014**, *118*, 1240–1247. [CrossRef]
35. Asano, K.; Enoki, H.; Akiba, E. Effect of Li Addition on Synthesis of Mg-Ti BCC Alloys by means of Ball Milling. *Mater. Trans.* **2007**, *48*, 121–126. [CrossRef]
36. Vermeulen, P.; van Thiel, E.F.; Notten, P.H. Ternary MgTiX-alloys: A promising route towards low-temperature, high-capacity, hydrogen-storage materials. *Chemistry* **2007**, *13*, 9892–9898. [CrossRef]
37. Jain, A.; Miyaoka, H.; Ichikawa, T. Destabilization of lithium hydride by the substitution of group 14 elements: A review. *Int. J. Hydrog. Energy* **2016**, *41*, 5969–5978. [CrossRef]
38. Bloch, J. The kinetics of a moving metal hydride layer. *J. of Alloys Compd.* **2000**, *312*, 135–153. [CrossRef]
39. Wang, C.S.; Wang, X.H.; Lei, Y.Q.; Chen, C.P.; and Wang, Q.D. Hydriding Kinetics of M1Ni-I Development of the model. *Int. J. Hydrog. Energy* **1996**, *21*, 471–478. [CrossRef]
40. Du, A.J.; Smith, S.C.; Yao, X.D.; Lu, G.Q. Hydrogen spillover mechanism on a Pd-doped Mg surface as revealed by ab initio density functional calculation. *J. Am. Chem. Soc.* **2007**, *129*, 10201–10204. [CrossRef]
41. Yao, X.; Wu, C.; Du, A.; Zou, J.; Zhu, Z.; Wang, P.; Cheng, H.; Smith, S.C.; Lu, G. Metallic and carbon nanotube-catalyzed coupling of hydrogenation in magnesium. *J. Am. Chem. Soc.* **2007**, *129*, 15650–15654. [CrossRef]
42. Pan, Y.-C.; Zou, J.-X.; Zeng, X.-Q.; Ding, W.-J. Hydrogen storage properties of Mg–TiO_2 composite powder prepared by arc plasma method. *Trans. Nonferrous Met. Soc. China* **2014**, *24*, 3834–3839. [CrossRef]

43. Liu, H.; Sun, P.; Bowman, R.C.; Fang, Z.Z.; Liu, Y.; Zhou, C. Effect of air exposure on hydrogen storage properties of catalyzed magnesium hydride. *J. Power Sources* **2020**, *454*, 227936. [CrossRef]
44. Ma, T.; Isobe, S.; Wang, Y.; Hashimoto, N.; Ohnuki, S. Nb-Gateway for Hydrogen Desorption in Nb_2O_5 Catalyzed MgH_2 Nanocomposite. *J. Phys. Chem. C* **2013**, *117*, 10302–10307. [CrossRef]
45. Lu, C.; Ma, Y.; Li, F.; Zhu, H.; Zeng, X.; Ding, W.; Wu, J.; Deng, T.; Zou, J. Visualization of fast "hydrogen pump" in core-shell nanostructured Mg@Pt through hydrogen stabilized Mg_3Pt. *J. Mater. Chem. A* **2019**, *24*, 14629–14637. [CrossRef]
46. Zhou, C.; Fang, Z.Z.; Sun, P. An experimental survey of additives for improving dehydrogenation properties of magnesium hydride. *J. Power Sources* **2015**, *278*, 38–42. [CrossRef]
47. Rizo-Acosta, P.; Cuevas, F.; Latroche, M. Hydrides of early transition metals as catalysts and grain growth inhibitors for enhanced reversible hydrogen storage in nanostructured magnesium. *J. Mater. Chem. A* **2019**, *7*, 23064–23075. [CrossRef]
48. Charbonnier, J.; de Rango, P.; Fruchart, D.; Miraglia, S.; Pontonnier, L.; Rivoirard, S.; Skryabina, N.; Vulliet, P. Hydrogenation of transition metal additives (Ti, V) during ball milling of Magnesium Hydride. *J. Alloys Compds* **2004**, *383*, 205–208. [CrossRef]
49. Lu, H.B.; Poh, C.K.; Zhang, L.C.; Guo, Z.P.; Yu, X.B.; Liu, H.K. Dehydrogenation characteristics of Ti- and Ni/Ti-catalyzed Mg hydrides. *J. Alloys Compd.* **2009**, *481*, 152–155. [CrossRef]
50. Shahi Rohit, R.; Tiwari Anand, P.; Shaz, M.A.; Srivastava, O.N. Studies on de/rehydrogenation characteristics of nanocrystalline MgH_2 co-catalyzed with Ti, Fe and Ni. *Int. J. Hydrog. Energy* **2013**, *38*, 2778–2784. [CrossRef]
51. Wang, Y.; Zhang, Q.; Wang, Y.; Jiao, L.; Yuan, H. Catalytic effects of different Ti-based materials on dehydrogenation performances of MgH_2. *J. Alloys Compd.* **2015**, *645*, S509–S512. [CrossRef]
52. Choi, Y.J.; Lu, J.; Sohn, H.Y.; Fang, Z.Z. Hydrogen storage properties of the Mg-Ti-H system prepared by high-energy-high-pressure reactive milling. *J. Power Sources* **2008**, *180*, 491–497. [CrossRef]
53. Choi, Y.J.; Jun, L.; Hong, Y.; Zhigang, Z.F.; Ewa, R. Effect of Milling Parameters on the Dehydrogenation Properties of the Mg-Ti-H System. *J. Phys. Chem. C* **2009**, *130*, 19344–19350. [CrossRef]
54. Lu, J.; Choi, Y.J.; Fang, Z.Z.; Sohn, H.Y.; Ronnebro, E. Hydrogen Storage Properties of Nanosized MgH_2-0.1TiH_2 Prepared by Ultrahigh-Energy-High-Pressure Milling. *J. Am. Chem. Soc.* **2009**, *131*, 15843–15852. [CrossRef] [PubMed]
55. Lu, J.; Choi, Y.J.; Fang, Z.Z.; Sohn, H.Y.; Roennebro, E. Hydrogenation of Nanocrystalline Mg at Room Temperature in the Presence of TiH_2. *J. Am. Chem. Soc.* **2010**, *132*, 6616–6617. [CrossRef] [PubMed]
56. Patelli, N.; Migliori, A.; Pasquini, L. Reversible metal-hydride transformation in Mg-Ti-H nanoparticles at remarkably low temperatures. *ChemPhysChem* **2019**, *20*, 1325–1333. [CrossRef]
57. Choi, E.; Song, M.Y. Hydriding and dehydriding features of a titanium-added magnesium hydride composite. *Mat. Sci.* **2020**, *26*, 199–204. [CrossRef]
58. Lotoskyy, M.; Denys, R.; Yartys, V.A.; Eriksen, J.; Goh, J.; Nyamsi, S.N.; Sita, C.; Cummings, F. An outstanding effect of graphite in nano-MgH_2-TiH_2 on hydrogen storage performance dagger. *J. Mater. Chem. A* **2018**, *6*, 10740–10754. [CrossRef]
59. Cuevas, F.; Korablov, D.; Latroche, M. Synthesis, structural and hydrogenation properties of Mg-rich MgH_2–TiH_2 nanocomposites prepared by reactive ball milling under hydrogen gas. *Phys. Chem. Chem. Phys.* **2012**, *14*, 1200–1211. [CrossRef]
60. Shao, H.; Felderhoff, M.; Schuth, F. Hydrogen storage properties of nanostructured MgH_2/TiH_2composite prepared by ball milling under high hydrogen pressure. *Int. J. Hydrog. Energy* **2011**, *36*, 10828–10838. [CrossRef]
61. Pasquini, L.; Callini, E.; Brighi, M.; Boscherini, F.; Montone, A.; Jensen, T.R.; Maurizio, C.; Antisari, M.V.; Bonetti, E. Magnesium nanoparticles with transition metal decoration for hydrogen storage. *J. Nanopart. Res.* **2011**, *13*, 5727–5737. [CrossRef]
62. Vincent, S.; Lang, J.; Huot, J. Addition of catalysts to magnesium hydride by means of cold rolling. *J. Alloys Compd.* **2012**, *512*, 290–295. [CrossRef]
63. Ma, L.-P.; Wang, P.; Kang, X.-D.; Cheng, H.-M. Preliminary investigation on the catalytic mechanism of TiF_3 additive in MgH_2–TiF_3 H-storage system. *J. Mater. Res.* **2011**, *22*, 1779–1786. [CrossRef]
64. Zhou, C.; Fang, Z.Z.; Ren, C.; Li, J.; Lu, J. Effect of Ti Intermetallic catalysts on hydrogen storage properties of magnesium hydride. *J. Phys. Chem. C* **2013**, *117*, 12973–12980. [CrossRef]
65. Choi, Y.J.; Choi, J.W.; Sohn, H.Y.; Ryu, T.; Hwang, K.S.; Fang, Z.Z. Chemical vapor synthesis of Mg–Ti nanopowder mixture as a hydrogen storage material. *Int. J. Hydrog. Energy* **2009**, *34*, 7700–7706. [CrossRef]
66. Cui, J.; Wang, H.; Liu, J.; Ouyang, L.; Zhang, Q.; Sun, D.; Yao, X.; Zhu, M. Remarkable enhancement in dehydrogenation of MgH_2 by a nano-coating of multi-valence Ti-based catalysts. *J. Mater. Chem. A* **2013**, *492*, 251–258. [CrossRef]
67. Calizzi, M.; Venturi, F.; Ponthieu, M.; Cuevas, F.; Morandi, V.; Perkisas, T.; Bals, S.; Pasquini, L. Gas-phase synthesis of Mg–Ti nanoparticles for solid-state hydrogen storage. *Phys. Chem. Chem. Phys.* **2016**, *18*, 141–148. [CrossRef] [PubMed]
68. Lu, C.; Zou, J.; Shi, X.; Zeng, X.; Ding, W. Synthesis and hydrogen storage properties of core–shell structured binary Ti and ternary Ni composites. *Int. J. Hydrog. Energy* **2017**, *42*, 2239–2247. [CrossRef]
69. Liu, T.; Chen, C.; Wang, F.; Li, X. Enhanced hydrogen storage properties of magnesium by the synergic catalytic effect of TiH1.971 and TiH1.5 nanoparticles at room temperature. *J. Power Sources* **2014**, *267*, 69–77. [CrossRef]
70. Manivasagam, T.G.; Magusin, P.C.M.M.; Iliksu, M.; Notten, P.H.L. Influence of Nickel and Silicon Addition on the Deuterium Siting and Mobility in fcc Mg–Ti Hydride Studied with $_2$H MAS NMR. *J. Phys. Chem. C* **2014**, *118*, 10606–10615. [CrossRef]
71. Yu, H.; Zhang, S.; Zhao, H.; Will, G.; Liu, P. An efficient and lowcost TiO_2 compact layer for performance improvement of dye-sensitized solar cells. *Electrochim. Acta* **2009**, *54*, 1319–1324. [CrossRef]

72. Polanski, M.; Bystrzycki, J. Comparative studies of the influence of different nano-sized metal oxides on the hydrogen sorption properties of magnesium hydride. *J. Alloys Compd.* **2009**, *486*, 697–701. [CrossRef]
73. Pramoch, R.; Pattaraporn, S.; Boonyarach, K.; Santi, K. Effects of $TiCl_3$, TiO_2, $ZrCl_4$, and ZrO_2 on Hydrogen Desorption of MgH_2 and Its Reversibility. *Chem. Eng. Trans.* **2014**, *39*, 1201–1206.
74. Zhang, M.; Xiao, X.; Luo, B.; Liu, M.; Chen, M.; Chen, L. Superior de/hydrogenation performances of MgH_2 catalyzed by 3D flower-like TiO_2@C nanostructures. *J. Energy Chem.* **2020**, *46*, 191–198. [CrossRef]
75. Pandey, S.K.; Bhatnagar, A.; Shahi, R.R.; Hudson, M.S.L.; Singh, M.K.; Srivastava, O.N. Effect of TiO_2 nanoparticles on the hydrogen sorption characteristics of magnesium hydride. *J. Nanosci. Nanotechnol.* **2013**, *13*, 5493–5499. [CrossRef]
76. Daryani, M.; Simchi, A.; Sadati, M.; Mdaah Hosseini, H.; Targholizadeh, H.; Khakbiz, M. Effects of Ti-based catalysts on hydrogen desorption kinetics of nanostructured magnesium Hydride. *Int. J. Hydrog. Energy.* **2014**, *39*, 21007–21014. [CrossRef]
77. Mirabile Gattia, D.; Di Girolamo, G.; Montone, A. Microstructure and kinetics evolution in MgH_2–TiO_2 pellets after hydrogen cycling. *J. Alloys Compd.* **2014**, *615*, S689–S692. [CrossRef]
78. Jung, K.S.; Kim, D.H.; Lee, E.Y.; Lee, K.S. Hydrogen sorption of magnesium hydride doped with nano-sized TiO_2. *Catal. Today* **2007**, *120*, 270–275. [CrossRef]
79. Vujasin, R.; Mrakovic, A.; Kurko, S.; Novakovic, N.; Matovic, L.; Novakovic, J.G.; Milosevic, S. Catalytic activity of titania polymorphs towards desorption reaction of MgH_2. *Int. J. Hydrog. Energy.* **2016**, *41*, 4703–4711. [CrossRef]
80. Zhang, X.; Leng, Z.; Gao, M.; Hu, J.; Fang, D.; Yao, J.; Pan, H.; Liu, Y. Enhanced hydrogen storage properties of MgH_2 catalyzed with carbon-supported nanocrystalline TiO_2. *J. Power Sources* **2018**, *398*, 183–192. [CrossRef]
81. Berezovets, V.; Denys, R.; Zavaliy, I.; Kosarchyn, Y. Effect of Ti-based nanosized additives on the hydrogen storage properties of MgH_2. *Int. J. Hydrog. Energy* **2022**, *47*, 2789–7298. [CrossRef]
82. Oelerich, W.; Klassen, T.; Bormann, R. Mg-based hydrogen storage materials with improved hydrogen sorption. *Mater. Trans* **2001**, *42*, 1588–1592. [CrossRef]
83. Wang, P.; Wang, A.; Zhang, H.; Ding, B.; Hu, Z. Hydrogenation characteristics of Mg–TiO (rutile) composite. *J. Alloys Compd.* **2000**, *313*, 218–223. [CrossRef]
84. Chen, M.; Xiao, X.; Zhang, M.; Liu, M.; Huang, X.; Zheng, J.; Zhang, Y.; Jiang, L.; Chen, L. Excellent synergistic catalytic mechanism of in-situ formed nanosized Mg_2Ni and multiple valence titanium for improved hydrogen desorption properties of magnesium hydride. *Int. J. Hydrog. Energy.* **2019**, *44*, 1750–1759. [CrossRef]
85. Jangir, M.; Mirabile Gattia, D.; Peter, A.; Jain, I.P. Effect of Ti-Additives on Hydrogenation/Dehydrogenation Properties of MgH_2. In Proceedings of the AIP Conference Proceeding, Rome, Italy, 11–14 September 2019; Volume 2145.
86. Liu, G.; Wang, L.; Hu, Y.; Sun, C.; Leng, H.; Li, Q.; Wu, C. Enhanced catalytic effect of TiO_2@rGO synthesized by one-pot ethylene glycol-assisted solvothermal method for MgH_2. *J. Alloys Compd.* **2021**, *881*, 160644. [CrossRef]
87. Jin, S.-A.; Ahn, J.-P.; Shim, J.-H.; Cho, Y.W.; Yi, K. Dehydrogenation and hydrogenation characteristics of MgH_2 with transition metal fluorides. *J. Power Sources* **2007**, *172*, 859–862. [CrossRef]
88. Deledda, S.; Borissova, A.; Poinsignon, C.; Botta, W.; Dornheim, J.; Klassen, M. H-sorption in MgH_2 nanocomposites containing Fe or Ni with fluorine. *J. Alloys Compd.* **2005**, *404*, 409–412. [CrossRef]
89. de Castro, J.F.R.; Yavari, A.R.; LeMoulec, A.; Ishikawa, T.T.; Botta, W.J. Improving H-sorption in MgH_2 powders by addition of nanoparticles of transition metal fluoride catalysts and mechanical alloying. *J. Alloys Compd.* **2005**, *389*, 270–274. [CrossRef]
90. Yavari, A.R.; LeMoulec, A.; de Castro, J.F.R.; Deledda, S.; Friedrichs, O.; Botta, W.J. Improvement in H- sorption kinetics of MgH_2 powders by using Fe nanoparticles generated by reactive FeF_3 addition. *Scr. Mater.* **2005**, *52*, 719–724. [CrossRef]
91. Kim, J.W.; Ahn, J.-P.; Jin, S.-A.; Lee, S.H.; Chung, H.-S.; Shim, J.-H. Microstructural evolution of NbF_5-doped MgH_2 exhibiting fast hydrogen sorption kinetics. *J. Power Sources* **2008**, *178*, 373–378. [CrossRef]
92. Ma, L.-P.; Kang, X.-D.; Dai, H.-B.; Liang, Y.; Fang, Z.-Z.; Wang, P.J. Superior catalytic effect of TiF_3 over $TiCl_3$ in improving the hydrogen sorption kinetics of MgH_2: Catalytic role of fluorine anion. *Acta Mater.* **2009**, *57*, 2250–2258. [CrossRef]
93. Malka, I.E.; Czujko, T.; Bystrzycki, J. Catalytic effect of halide additives ball milled with Magnesium hydride. *Int. J. Hydrog. Energy.* **2010**, *35*, 1706–1712. [CrossRef]
94. Peng, S.-K.; Xiao, X.-Z.; Xu, R.-J.; Li, L.; Wu, F.; Li, S.-Q.; Wang, Q.-D.; Chen, L.-X. Hydrogen storage behaviours and microstructure of MF_3 (M = Ti, Fe)-doped magnesium hydride. Trans. *Nonferrous Met. Soc.* **2010**, *20*, 1879–1884. [CrossRef]
95. Jangir, M.; Jain, A.; Yamaguchi, S.; Ichikawa, T.; Lal, C.; Jain, I.P. Catalytic effect of TiF_4 in improving hydrogen storage properties of MgH_2. *Int. J. Hydrog. Energy.* **2016**, *41*, 14178–14183. [CrossRef]
96. Ma, L.-P.; Wang, P.; Cheng, H.-M. Improving hydrogen sorption kinetics of MgH_2 by mechanical milling with TiF_3. *J. Alloys Compd.* **2007**, *432*, L1–L4. [CrossRef]
97. Danaie, M.; Mitlin, D. TEM analysis of the microstructure in TiF_3-catalyzed and pure MgH_2 during the hydrogen storage cycling. *Acta Mater.* **2012**, *60*, 6441–6456. [CrossRef]
98. Mustafa, N.S.; Ismai, M. Influence of K_2TiF_6 additive on the hydrogen sorption properties of MgH_2. *Int. J. Hydrog. Energy* **2014**, *39*, 15563–15569. [CrossRef]
99. Jain, A.; Agarwal, S.; Kumar, S.; Yamaguchi, S.; Miyaoka, H.; Kojima, Y.; Ichikawa, T. How does TiF_4 affect the decomposition of MgH_2 and its complex variants?—An XPS investigation. *J. Mater. Chem. A* **2017**, *5*, 15543–15551. [CrossRef]
100. Guoxian, L.; Erde, W.; Shoushi, F. Hydrogen absorption and desorption characteristics of mechanically milled Mg-35 wt% $FeTi_{1.2}$ powders. *J. Alloys Compd.* **1995**, *223*, 111–114. [CrossRef]

101. Meena, P.; Jangir, M.; Singh, R.; Sharma, V.K.; Jain, I.P. Hydrogen kinetics studies of MgH_2-FeTi composites. *AIP Conf. Proc.* **2018**, *1*, 030010.
102. Lal, C.; Singh, V.; Jangir, M.; Jain, R.K.; Jain, I.P. Evolution of microstructure of Mg + FeTi nanocomposite prepared by mechanical alloying. *AIP Conf. Proc.* **2013**, *1536*, 883–884.
103. Reule, H.; Hirscher, M.; Weißhardt, A.; Kronmüller, H. Hydrogen desorption properties of mechanically alloyed MgH_2 composite materials. *J. Alloys Compd.* **2000**, *305*, 246–252. [CrossRef]
104. Cui, N.; Luan, B.; Zhao, H.; Liu, H.K.; Dou, S.X. Synthesis and electrode characteristics of the new composite alloys Mg_2Ni-xwt%Ti_2Ni. *J. Alloys Compd.* **1996**, *240*, 229–234. [CrossRef]
105. Hu, Y.; Zhang, H.; Wang, A.; Ding, B.; Hu, Z. Preparation and hydriding/dehydriding properties of mechanically milled Mg–30 wt% $TiMn_{1.5}$ composite. *J. Alloys Compd.* **2003**, *354*, 296–302. [CrossRef]
106. El-Eskandarany, M.S.; Shaban, E.; Aldakheel, F.; Alkandary, A.; Behbehani, M.; Al-Saidi, M. Synthetic nanocomposite MgH_2/5 wt.% $TiMn_2$ powders for solid-hydrogen storage tank integrated with PEM fuel cell. *Sci. Rep.* **2017**, *7*, 13296. [CrossRef]
107. El-Eskandarany, M.S.; Al-Ajmi, F.; Banyan, M.; Al-Duweesh, A. Synergetic effect of reactive ball milling and cold pressing on enhancing the hydrogen storage behavior of nanocomposite MgH2/10 wt% TiMn2 binary system. *Int. J. Hydrog. Energy* **2019**, *44*, 26428–26443. [CrossRef]
108. Dai, J.H.; Jiang, X.W.; Song, Y. Stability and hydrogen adsorption properties of Mg/$TiMn_2$ interface by first principles calculation. *Surf. Sci.* **2016**, *653*, 22–26. [CrossRef]
109. Kalisvaart, W.; Harrower, C.; Haagsma, J.; Zahiri, B.; Luber, E.; Ophus, C.; Poirier, E.; Fritzsche, H.; Mitlin, D. Hydrogen storage in binary and ternary Mg-based alloys: A comprehensive experimental study. *Int. J. Hydrog. Energy* **2010**, *35*, 2091–2103. [CrossRef]
110. Zahiri, B.; Amirkhiz, B.S.; Mitlin, D. Hydrogen storage cycling of MgH_2 thin film nanocomposites catalyzed by bimetallic Cr Ti. *Appl. Phys. Lett.* **2010**, *97*, 083106. [CrossRef]
111. Wu, Z.; Fang, J.; Liu, N.; Wu, J.; Kong, L. The Improvement in Hydrogen Storage Performance of MgH_2 Enabled by Multilayer Ti_3C_2. *Micromachines* **2021**, *12*, 1190. [CrossRef]
112. Li, J.; Wang, S.; Du, Y.; Liao, W. Catalytic effect of Ti_2C MXene on the dehydrogenation of MgH_2. *Int. J. Hydrog. Energy* **2019**, *44*, 6787–6794. [CrossRef]
113. Liu, Y.; Gao, H.; Zhu, Y.; Li, S.; Zhang, J.; Li, L. Excellent catalytic activity of a two-dimensional $Nb_4C_3T_x$ (MXene) on hydrogen storage of MgH_2. *Appl. Surf. Sci.* **2019**, *493*, 431–440. [CrossRef]
114. Zhu, W.; Panda, S.; Lu, C.; Ma, Z.; Khan, D.; Dong, D.; Sun, F.; Xu, H.; Zhang, Q.; Zou, J. Using a Self-Assembled Two-Dimensional MXene-Based Catalyst (2D-Ni@Ti_3C_2) to Enhance Hydrogen Storage Properties of MgH_2. *ACS Appl Mater Interfaces* **2020**, *12*, 50333–50343. [CrossRef]
115. Huang, T.; Huang, X.; Hu, C.; Wang, J.; Liu, H.; Xu, H.; Sun, F.; Ma, Z.; Zou, J.; Ding, W. MOF-derived Ni nanoparticles dispersed on monolayer MXene as catalyst for improved hydrogen storage kinetics of MgH_2. *Chem. Eng. J.* **2021**, *421*, 127851. [CrossRef]
116. Zhu, W.; Ren, L.; Lu, C.; Xu, H.; Sun, F.; Ma, Z.; Zou, J. Nanoconfined and in Situ Catalyzed MgH_2 Self-Assembled on 3D Ti_3C_2 MXene Folded Nanosheets with Enhanced Hydrogen Sorption Performances. *ACS Nano* **2021**, *15*, 18494–18504. [CrossRef]
117. Kong, Q.; Zhang, H.; Yuan, Z.; Liu, J.; Li, L.; Fan, Y.; Fan, G.; Liu, B. Hamamelis-like $K_2Ti_6O_{13}$ Synthesized by Alkali Treatment of Ti_3C_2 MXene: Catalysis for Hydrogen Storage in MgH_2. *ACS Sustain. Chem. Eng.* **2020**, *8*, 4755–4763. [CrossRef]
118. Wang, Y.; Fan, G.; Zhang, D.; Fan, Y.; Liu, B. Striking enhanced effect of PrF_3 particles on Ti_3C_2 MXene for hydrogen storage properties of MgH_2. *J. Alloys Compd.* **2022**, *914*, 165291. [CrossRef]
119. Shen, Z.; Wang, Z.; Zhang, M.; Gao, M.; Hu, J.; Du, F.; Liu, Y.; Pan, H. A novel solid-solution MXene $(Ti_{0.5}V_{0.5})_3C_2$ with high catalytic activity for hydrogen storage in MgH_2. *Materialia* **2018**, *1*, 114–120. [CrossRef]
120. Gao, H.; Liu, Y.; Zhu, Y.; Zhang, J.; Li, L. Catalytic effect of sandwich-like Ti_3C_2/TiO_2(A)-C on hydrogen storage performance of MgH_2. *Nanotechnology* **2020**, *31*, 115404. [CrossRef]
121. Liu, H.Z.; Lu, C.L.; Wang, X.C.; Xu, L.; Huang, X.T.; Wang, X.H.; Ning, H.; Lan, Z.Q.; Guo, J. Combinations of V_2C and Ti_3C_2 MXenes for Boosting the Hydrogen Storage Performances of MgH_2. *ACS Appl. Mater. Interfaces* **2021**, *13*, 13235–13247. [CrossRef]
122. Chen, G.; Zhang, Y.; Cheng, H.; Zhu, Y.; Li, L.; Lin, H. Effects of two-dimension MXene Ti_3C_2 on hydrogen storage performances of MgH_2-$LiAlH_4$ composite. *Chem. Phys.* **2019**, *522*, 178–187. [CrossRef]
123. Huang, X.; Lu, C.; Li, Y.; Tang, H.; Duan, X.; Wang, K.; Liu, H. Hydrogen Release and Uptake of MgH_2 Modified by Ti_3CN MXene. *Inorganics* **2023**, *11*, 243. [CrossRef]
124. El-Eskandarany, M.S.; Shaban, E. Contamination Effects on Improving the Hydrogenation/Dehydrogenation Kinetics of Binary Magnesium Hydride/Titanium Carbide Systems Prepared by Reactive Ball Milling. *Materials* **2015**, *8*, 6880–6892. [CrossRef]
125. Khalil, R.M.A.; Hussain, F.; Imran, M.; Rasheed, U.; Rana, A.M.; Murtaza, G. An ab initio study of spectroscopic and thermodynamic characteristics of MgH_2 and TiC systems. *Int. J. Hydrog. Energy* **2019**, *44*, 6756–6762. [CrossRef]
126. Tian, Z.; Wang, Z.; Yao, P.; Xia, C.; Yang, T.; Li, Q. Hydrogen storage behaviors of magnesium hydride catalyzed by transition metal carbides. *Int. J. Hydrog. Energy* **2021**, *46*, 40203–40216. [CrossRef]
127. Sazelee, N.; Md Din, M.F.; Ismail, M.; Rather, S.-U.; Bamufleh, H.S.; Alhumade, H.; Taimoor, A.A.; Saeed, U. Effect of $LaCoO_3$ Synthesized via Solid-State Method on the Hydrogen Storage Properties of MgH_2. *Materials* **2023**, *16*, 2449. [CrossRef] [PubMed]
128. Yang, X.; Zhang, J.; Hou, Q.; Guo, X. Regulation of Kinetic Properties of Chemical Hydrogen Absorption and Desorption by Cubic K_2MoO_4 on Magnesium Hydride. *Nanomaterials* **2022**, *12*, 2468. [CrossRef]

129. El-Eskandarany, M.S.; Al-Ajmi, F.; Banyan, M. Mechanically-Induced Catalyzation of MgH_2 Powders with Zr_2Ni-Ball Milling Media. *Catalysts* **2019**, *9*, 382. [CrossRef]
130. An, C.; Deng, Q. Improvement of Hydrogen Desorption Characteristics of MgH_2 with Core-shell Ni@C Composites. *Molecules* **2018**, *23*, 3113. [CrossRef]